Published in final edited form as:
Mol Pharm. 2012 February 6; 9(2): 201–210. doi:10.1021/mp200426h.

SPANosomes as delivery vehicles for small interfering RNA (siRNA)

Chenguang Zhou[†,‡], **Yicheng Mao**[†,‡], **Yasuro Sugimoto**[§], **Yue Zhang**[†,¶], **Naveen Kanthamneni**[†], **Bo Yu**[‡,‖], **Robert W. Brueggemeier**[§], **L. James Lee**[‡,‖], and **Robert J. Lee**[†,‡,*]

[†]Division of Pharmaceutics, College of Pharmacy, The Ohio State University, Columbus, OH 43210, United States

[‡]NSF Nanoscale Science and Engineering Center (NSEC) for Affordable Nanoengineering of Polymeric Biomedical Devices (CANPBD), The Ohio State University, Columbus, OH 43210, United States

[§]Division of Medicinal Chemistry & Pharmacognosy, College of Pharmacy, The Ohio State University, Columbus, OH 43210, United States

[‖]Department of Chemical and Biomolecular Engineering, The Ohio State University, Columbus, OH 43210, USA

[¶]College of Pharmacy, Nankai University, Tianjin, China, 300071

Abstract

Non-ionic surfactant vesicles, or SPANosomes (SPs), comprised of cationic lipid and sorbitan monooleate (Span 80) were synthesized and evaluated as siRNA vectors. The SPs had a mean diameter of less than 100 nm and exhibited excellent colloidal stability. The SP/siRNA complexes possessed a slightly positive zeta potential of 12 mV and demonstrated a high siRNA incorporation efficiency of greater than 80%. Cryogenic transmission electron microscopy (cryo-TEM) imaging of the SP/siRNA indicated a predominantly core-shell structure. The SP/siRNA complexes were shown to efficiently and specifically silence expression of both green fluorescent protein (GFP) (66% knockdown) and aromatase (77% knockdown) genes in breast cancer cell lines. In addition, the cellular trafficking pathway of the SP/siRNA was investigated by confocal microscopy using molecular beacons as probes for cytosolic delivery. The results showed efficient endosomal escape and cytosolic delivery of the siRNA cargo following internalization of the SP/siRNA complexes. In conclusion, Span 80 is a potent helper lipid and the SPs are promising vehicles for siRNA delivery.

Keywords

Drug delivery; Nanoparticles; Surfactant vesicles; siRNA; Molecular beacon

1 Introduction

RNA interference (RNAi) is a potent and highly specific strategy for silencing gene expression[1]. siRNAs have been investigated as therapeutic agents for the treatment of hypercholesterolemia[2], viral infection[3], cancer[4], and other diseases[5]. However, the polyanionic and hydrophilic nature of siRNA duplexes prevent them from crossing the cell

[*]Corresponding author: Robert J. Lee, College of Pharmacy, 500 W. 12th Avenue, Columbus, OH 43210. Telephone: 614-292-4172; Fax: 614-292-7766; lee.1339@osu.edu.

membrane. An effective delivery system is, therefore required to maximize their therapeutic value[1].

Both nonviral and viral vectors have been developed for therapeutic applications in RNAi[6, 7]. Among non-viral vectors, cationic liposomes are the most studied[6]. Considerable effort has been invested in developing novel cationic lipids for siRNA delivery[8]. In contrast, less attention has been given to developing more effective helper lipids[9, 10]. Non-ionic surfactants such as Span 80 are able to self-assemble into vesicles in aqueous medium[11] and possess a bilayer structure similar to that of liposomes. Surfactant vesicles have been investigated as alternatives to liposomes as carriers of anticancer drugs[12], X-ray contrast agents[13], and antigens for vaccination[14]. More recently, non-ionic surfactants have been incorporated into cationic liposomes as helper component for the delivery of plasmid DNA and oligodeoxyribonucleotides (ODN)[15, 16]. However, non-ionic surfactants have yet to be characterized in siRNA carriers.

In this study, Span 80 surfactant vesicles called SPANosomes (SPs) were synthesized and evaluated as siRNA vectors. SPs are composed of Span 80, 1,2-dioleoyl-3-trimethylammonium-propane (DOTAP), and D-α-tocopheryl polyethylene glycol-1000 succinate (TPGS). The transfection activity, structure, and intracellular trafficking of SP/siRNA complexes were investigated.

2 Materials and Methods

2.1 Material

DOTAP was purchased from Genzyme Pharmaceuticals (Cambridge, MA). Span 80 and TPGS were obtained from Fisher Scientific Inc. (Pittsburgh, PA). 7α-(4'-Amino) phenylthio-1,4-androstadiene-3,17-dione (7α-APTADD) was synthesized by Dr. Michael Darby as described previously[17]. CellTiter 96® AQueous One Solution Cell Proliferation (MTS) Assay kits were purchased from Promega (Madison, WI). The Silencer® eGFP siRNA (siGFP) and Negative Control #1 siRNA (siNC), Lipofectamine 2000 (LF), Silencer® Cy3 labeled Negative Control #1 siRNA (Cy3-siRNA), FAM™-Labeled Negative Control #1 siRNA (FAM-siRNA), b-medium, LysoSensor™ Green DND-189, and Quant-iT™ RiboGreen® RNA Reagent were purchased from Invitrogen (Carlsbad, CA). Sucrose, LY29004, and filipin III were purchased from Sigma-Aldrich Chemical Co. (St. Louis, MO, USA). The sense and antisense strands of siRNA targeting the aromatase gene (siArom) were 5'-CGGUAUGCAUGAGAAAGGCAUCAUA-3' and 5'-UAUGAUGCCUUUCUCAUGCAUACCG-3' respectively. The sequence of the control siRNA sense and antisense strands (siCTRL) were 5'-CGGGUACGUGAAAGACGUACAUAUA-3' and 5'-UAUAUGUACGUCUUUCACGUACCCG-3' respectively. SiArom and siCTRL were synthesized by Invitrogen (Carlsbad, CA). The GAPDH mRNA targeting molecular beacon (MB) had the sequence of 5'-Cy3-CGACGGAGTCCTTCCACGATACCACGTCG-BHQ2-3' and was synthesized by Eurofins MWG Operon (Huntsville, AL). Negative control siRNA (5'-UUCUCCGAACGUGUCACGUTT-3', 5'-ACGUGACACGUUCGGAGAATT-3') were synthesized by GenePharma Co., Ltd (Shanghai, China) and used for particle size, zeta potential, and incorporation test. All reagents were of analytical grade and used without further purification.

2.2 Synthesis of SPs

The SP formulations, composed of DOTAP, Span 80, and TPGS, were prepared by ethanol injection method[18, 19]. Briefly, stock solutions were prepared by dissolving 50 mg/ml lipid or surfactant component in 100% ethanol. These were then combined at the desired molar

ratios (Table 1). Unless otherwise specified, all experiments were carried out with SPs containing 1% TPGS. To synthesize the SPs, a 40 μl ethanol solution of lipid and surfactant mixture was rapidly injected into 960 μl calcium acetate buffer (18.75 mM, pH=6.8) followed by 30s of vortex mixing at room temperature. The final calcium acetate concentration was 18 mM and the total lipid/surfactant concentration was 2 mg/ml.

2.3 Optimization of the SP formulation

SP/siRNA complexes were prepared at a series of nucleic acid/SP (NA/SP, w/w) ratios as follows. Briefly, siRNA solution was mixed with SPs at various NA/SP ratios under vortexing. The SP/siRNA complexes were incubated at room temperature for 15 minutes and were then analyzed for particle size, zeta potential, and siRNA incorporation efficiency. Transfection efficiencies of the SP/siRNA complexes prepared at different NA/SP ratios were measured as described in section 2.7. The optimal NA/SP ratio of the SP formulation was determined based on particle size, zeta potential, and siRNA incorporation efficiency[20].

2.4 Characterization of SP/siRNA complexes

The particle sizes of SP or SP/siRNA complexes were determined by dynamic light-scattering (DLS) on a NICOMP Submicron Particle Sizer Model 370 (Santa Barbara, CA) in volume-weighted mode. The zeta potentials (ζ) of the complexes in 1.4 ml 0.1× PBS solution were determined on a ZetaPALS instrument (Brookhaven Instruments Corp., Worcestershire, NY). The siRNA incorporation efficiency was determined using the Quant-iT™ RiboGreen® RNA Kit[21] following the manufacturer's instructions. The siRNA incorporation efficiency was calculated using the equation:

$$\text{Incorportation efficiency}=(1-\frac{\text{Fluorescence without Triton X}-100}{\text{Fluorescence with Triton X}-100})\times 100\%.$$

2.5 Cryogenic transmission electron microscopy of SP/siRNA complexes

SP/siRNA complexes were prepared as described in section 2.3. The morphologies of the complexes were examined by cryo-TEM as described by Yang et al.[22]. The samples were viewed under a Tecnai G2 Transmission Electron Microscope (FEI Company, Oregon, USA) operating at 120 kV using a Gatan HC3500 Tilt heating/Nitrogen cooling holder (Pleasanton, CA, USA). Images were recorded digitally by a Gatan 791 MultiScan CCD camera and processed using the Digital Micrograph 3.1 software package. Further image processing was performed using the Paint.NET software package.

2.6 Cell culture

MDA-MB-231 cells with or without stably transfected green fluorescent protein (GFP) expression were grown in DMEM/F12 culture medium supplemented with 5% fetal bovine serum (FBS), 100 U/mL penicillin, and 100 μg/mL streptomycin, at 37 °C in a humidified atmosphere containing 5% CO_2.

The aromatase-expressing cell line SKBr-3 was maintained in b-medium supplemented with 10% FBS at 37 °C in a humidified atmosphere containing 5% CO_2.

2.7 In vitro transfection studies

MDA-MB-231-GFP cells, stably transfected with GFP, were used in studies involving siGFP. The cells were cultured until 80% confluence was reached and were seeded in a 24-well plate (6×10^4 cells/well) 1 day before transfection. For the transfection study, siRNA (siGFP or siNC) was combined with transfection vectors at NA/SP ratios of 5 to 20 in serum

free medium and incubated for about 15 min at room temperature. LF was used as a reference control for the transfection vector. The cells were incubated with siRNA complexes in 200 μl serum-free DMEM/F12 growth medium for 4 h at 37 °C. Then, the medium was replaced with fresh medium and the cells were incubated for a further 24 h followed by analysis of target gene expression.

GFP expression levels were quantified by flow cytometry. Briefly, the cells were rinsed three times with PBS (pH 7.4), detached with trypsin-EDTA, pelleted by centrifugation, and fixed with 500 μl 4% formalin in PBS. The cellular suspension samples were then analyzed a Becton Dickinson FACSCalibur cytometer (Becton Dickinson, Franklin Lakes, NJ) to determine the level of GFP expression. For each sample, > 1×10^5 events were collected. The data obtained was analyzed using BD CellQuest Pro software (Becton Dickinson, Franklin Lakes, NJ). The mean fluorescence intensity (MFI) of GFP was used to calculate the percentage of gene silencing (%) using the formula:

$$\text{Percentage of GFP silencing}=\left(1-\frac{\text{MFI of the transfected cells}}{\text{MFI of the untreated control cells}}\right)\times 100\%.$$

SKBr-3 cells were used in further studies involving aromatase gene silencing. The cells were seeded in b-medium supplemented with 10% FBS without antibiotics at a density of 1.5×10^5 cells/well in 6-well plates. After culturing overnight, the cells were treated with SP/siArom or SP/siCTRL complexes in OptiMEM. LF was used as a reference control for the transfection agent. After 6 hours of incubation, the medium was replaced with fresh b-medium supplemented with 10% FBS. After another 72 hours of incubation, aromatase activities were measured by the ^3H_2O release assay and the data obtained was normalized to the total DNA to determine normalized aromatase levels[23, 24]. The percentages of aromatase silencing were calculated by:

$$\text{Percentage of aromatase silencing}=\left(1-\frac{\text{normalized aromatase level of the transfected cells}}{\text{normalized aromatase level of the untreated control cells}}\right)\times 100\%$$

2.8 Subcellular distribution of siRNA

SPs with 1% TPGS or LF were complexed with Cy3-siRNA for transfection of MDA-MB-231 cells, as described above. The cells were seeded on round cover slips one day before transfection. The cells were transfected with SP/Cy3-siRNA or control LF/Cy3-siRNA complexes for 1 h in the presence of 2 μM LysoSensor Green DND-189. After transfection, the cells were washed 3 times with PBS and fixed in 4% formalin in PBS. Co-localization of Cy3-siRNA with the LysoSensor was analyzed on a Flowview 1000 Laser Scanning Confocal Microscope (Olympus).

2.9 Intracellular trafficking of siRNA

Intracellular trafficking of Cy3-siRNA and MB was investigated in MDA-MB-231 cells by flow cytometry analysis. For the studies, 6×10^4 cells were seeded in a 24-well plate one day before treatment. Cy3-siRNA or MB was complexed with SP or LF as described above. The cells were treated with complexes containing 100 nM Cy3-siRNA or MB for 2 h at 37 °C and were then washed three times with PBS, trypsinized, and fixed with 4% formalin. The resultant cellular fluorescent intensity was measured by flow cytometry on a Becton Dickinson FACSCalibur.

Specific endocytosis inhibitors were used to further delineate the mechanisms of SP and LF mediated siRNA transfection. MDA-MB-231 cells were seeded in a 24-well plate (6×10^4

cell/well) for 24 h. Before transfection, the cells were untreated or pre-incubated with an inhibitor of clathrin-mediated endocytosis (sucrose, 0.4 M), macropinocytosis (LY29004, 50 μM), or caveolae-mediated endocytosis (filipin III, 5 μg/ml) for 1 h at 37 °C[25–28]. The cells were then treated with 100 nM SP or LF/FAM-siRNA complexes for 1 h at 37 °C, washed three times with PBS, trypsinized, fixed with 4% formalin, and analyzed by flow cytometry. The MFI data obtained was normalized to the cells transfected with siRNA complexes in the absence of inhibitors.

2.10 Cytotoxicity assay

The vehicle related cytotoxicity of the SP fromulation was determined by the MTS assay[29]. MDA-MB-231 cells were seeded in 96-well plates at 5×10^3 cells/well one day before treatment. The cells were treated with different concentrations of SP diluted in DMEM growth medium. Following 24 h treatment, cell viability was accessed using the MTS assay according to the manufacturer's instructions. The absorption at 490 nm was measured on an automatic plate reader. Cell viability was expressed as a percentage of the untreated control based on absorption values at 490 nm.

2.11 Statistical analysis

The statistically significant differences were detected with Microsoft Excel 2003 software (Microsoft, Redmond, WA). Student's t-test was used to compare differences between two groups. Results were considered significant when p values were <0.05.

3 Results

3.1 Characteristics of SP formulations

SPs containing 1% or 5% TPGS were assessed for differences in particle size and zeta potential (Table 1). Inclusion of 5% TPGS resulted in a formulation that was smaller in size (~25 nm) compared to that with 1% TPGS (~40 nm). Due to the presence of DOTAP, the zeta potentials of both SP formulations were above +20 mV[30].

Figure 1 illustrates the effect of storage at 4 °C on the particle size of the SPs (containing 1% TPGS). There was only marginal increase in particle size during the three week period, indicating good colloidal stability of the SPs.

3.2 Optimization of the SP formulation

First, SP/siRNA complexes were prepared at different NA/SP ratios and their particle size and zeta potential were measured. As shown in Figure 2A, particle size and zeta potential changed according to the NA/SP ratio. A decrease in NA/SP ratio from 1/2.5 to 1/10 resulted in an increase in zeta potential from 8 mV to 13.7 mV. A further decrease of the NA/SP ratio to 1/15 resulted in a similar zeta potential of 12 mV. The size of SP/siRNA complexes was the smallest at 72 nm when synthesized at a NA/SP ratio of 1/15. The siRNA incorporation efficiency was found to be generally high across formulations (Figure 2B). Incorporation efficiency increased by reducing the NA/SP ratio, although the effect was minor. At the NA/SP ratio of 1/2.5, a 78% incorporation was attained, whereas at the NA/SP ratio of 1/15, 83% incorporation efficiency was achieved. Consequently, we chose 1/15 as the optimal NA/SP ratio since the complexes obtained exhibited a moderately positive zeta potential (12 mV), small particle size (~72 nm), and high siRNA incorporation efficiency (83%).

We next investigated the effect of TPGS as a PEGylating agent. TPGS added to the SP formulation at 1% or 5% had minimal effect on the zeta potential and incorporation efficiency (Figure 2B, C). The siRNA complexes of SPs with 5% TPGS showed a larger

particle size (109 nm) than those of SPs with 1% TPGS (72 nm). This difference in particle size may be due to random variability of the particles or batch-to-batch variability.

3.3 Cryo-TEM imaging of SP/siRNA complexes

The morphology of SP/siRNA complexes was analyzed by cryo-TEM (Figure 3), which has been extensively used in the study of liposome/siRNA complex morphology[31]. Figure 3A shows that SPs formed small size complexes with siRNA, which is consistent with our DLS measurements (Table 1). Unlike the multilamellar structures of liposome/siRNA complexes found in previous studies[31], SP/siRNA complexes are predominantly unilamellar core-shell particles (Figure 3B).

3.4 In vitro cytotoxicity assay

Vehicle related cytotoxicity of the SP formulation in MDA-MB-231 cells was studied using the MTS assay. The cells were treated with various amounts of SP formulation. As shown in Figure 4, the cytotoxicity increased as a function of SP concentration. SP concentration below 20 μg/ml (corresponding to a siRNA concentration of 100 nM) was well tolerated by cells, showing no significant cytotoxicity. When the SP concentration was increased to 100 μg/ml (corresponding to an siRNA concentration of 500 nM), significant cytotoxicity was observed. As a result, all the siRNA transfection experiments were carried out at SP concentrations less or equal to 20 μg/ml to avoid the confounding vehicle related cytotoxic effect on the gene silencing activity. The cytotoxicity observed may be due to the surfactant activities of Span 80[32] and DOTAP[33].

3.5 Gene silencing activity of the SP/siRNA complexes

Gene silencing study was performed on MDA-MB-231-GFP cells using SP/siGFP complexes. GFP silencing activity increased progressively as the NA/SP ratio decreased (Figure 5A) and was the greatest at the NA/SP ratio of 1/15. Decreasing the NA/SP ratio did not increase the silencing activity. The NA/SP ratio of 1/15 was therefore used in subsequent studies. SP/siNC complexes did not significantly affect GFP expression (Figure 5A). Together with the cytotoxicity data discussed above, these results demonstrated that the inhibition of GFP expression by the SP/siGFP complexes was through RNAi instead of vehicle related cytotoxic effect[31].

We further investigated the effect of siRNA dose on transfection activity. A cationic liposome based transfection reagent, LF, was used as a positive control[7, 34]. A clear dose dependence was shown for both SP/siGFP and LF/siGFP complexes (Figure 5C). At 40 nM siGFP, the SP complexes showed a 5.2-fold higher GFP silencing activity. SP/siGFP remained active at the 5 nM level, whereas the LF complexes lost activity at this level. The concentrations to attain 50% silencing by SP/siGFP and LF/siGFP complexes were estimated to be ~40 nM and ~120 nM, respectively, indicating a 3-fold higher siRNA transfection efficiency of SP complexes than that of LF.

It has been shown previously that incorporating a polyethylene glycol (PEG) based surfactant in cationic liposomes can improve their stability, but can decrease their transfection efficiency[35]. We investigated the transfection efficiency of SP containing TPGS, a PEG-containing surfactant. The results showed that SP/siGFP with 5% TPGS could still downregulate the GFP expression by 54%, which was slightly lower than the 66% knockdown obtained with SP containing 1% TPGS ($p>0.05$).

Next, we performed transfection experiments with siRNA targeting the endogenous aromatase gene in SKBr-3 cells. In Figure 6 results from aromatase activity assay indicate that the SP/siArom complexes are highly efficient for silencing the aromatase gene (77%

inhibition) at an siRNA concentration of 40 nM. The gene knockdown activity of the SP/siArom complexes was better than that of the LF. The SP/siArom with 5% TPGS was somewhat more effective in silencing the aromatase gene than those with 1% TPGS, but the difference was not statistically significant. Transfection with SP/siCTRL and LF/siCTRL complexes did not result in aromatase downregulation, suggesting that the inhibition of aromatase seen with the siArom complexes was due to RNAi.

3.6 Intracellular localization of siRNA

The intracellular localization of SP or LF/Cy3-siRNA (red) complexes was studied using confocal microscopy. The cells were treated with LysoTracker Green (green), a compound that primarily accumulates in cellular compartments with low internal pH[36], and siRNA complexes. Confocal microscopy images clearly showed extensive co-localization (yellow) of LF/siRNA complexes and LysoTracker Green. In contrast, SP/siRNA complexes did not significantly co-localize with LysoTracker Green (Figure 7). This revealed that SP/siRNA complexes were more capable of escaping from the acidic and nuclease rich environment of the lysosomes than LF/siRNA complexes[36].

3.7 Intracellular trafficking mechanism of the siRNA

Molecular beacons (MBs) are oligonucleotide probes that recognize and report the presence of specific mRNA sequences[37]. A MB has a fluorophore at one end and a quencher at the other end. They adopt a hairpin configuration in the absence of a target with a complementary sequence. When hybridized to a target, the quencher and the fluorophore are physically separated, allowing the fluorophore to emit fluorescence[38]. MBs have been used to track and locate endogenous mRNAs in living cells[39, 40]. While fluorescent signal of fluorescently labeled siRNA have been commonly used in quantification of siRNA delivery efficiency[20], the fluorescence signal, especially quantified by flow cytometry, does not differentiate those siRNA in endosomes/lysosomes and those in the cytosol. On the other hand, MBs become fluorescent only when bound to mRNA in the cytosol. Because MBs and siRNA are structural analogs, the fluorescence signal after cellular uptake of SP/MB complexes may be used to monitor the release of oligonucleotide payload into the cytosol. In addition, we have shown that the MFI of cells measured by flow cytometry have a linear relationship with amount of MB or fluorescently-labeled-siRNA content[40]. This provides a novel method for studying the cytosolic release of SP/siRNA and LF/siRNA complexes[40].

Transfection of Cy3-siRNA or MB complexes was studied in MDA-MB-231 cells to delineate the mechanism of siRNA delivery. Figure 8 shows that the MFIs in cells after treatment with free Cy3-siRNA or MB are low. This is because very limited amounts of free siRNA or MB can penetrate through the cell membrane due to their inherent hydrophilicity and high charge density[20]. Interestingly, the LF/Cy3-siRNA uptake was found to be significantly higher than that of the SP/Cy3-siRNA (Figure 8A, B). This result was contradictory to the GFP gene silencing data obtained, where SP/siGFP demonstrated a higher GFP silencing activity than LF/siGFP. The ratio of MFI_{MB} to $MFI_{Cy3\text{-}siRNA}$ indicates the portion of siRNA released into the cytosol. Our data showed that SP complexes released considerably higher portions of the nucleic acid cargo into the cytosol than those of LF (Figure 8B). This result was consistent with the results obtained by confocal microscopy, which also showed that the SP/siRNA complexes were able to escape from the lysosomal compartment more efficiently than the LF/siRNA complexes.

The effects of the specific endocytosis inhibitors on cellular uptake of siRNA complexes were quantified using flow cytometry analysis. Inhibitors for clathrin-mediated endocytosis (0.4 M sucrose solution), macropinocytosis inhibitor (50 μM LY29004), and the caveolae-mediated endocytosis inhibitor (5 μg/ml filipin III) were used to specifically inhibit

individual endocytic pathways. The uptake of SP/siRNA was inhibited by sucrose (43%), LY29004 (13%), and filipin III (61%) (Figure 9). In the case of LF, LY29004 did not inhibit LF uptake, while sucrose and filipin III reduced LF uptake by 62% and 35%, respectively (Figure 9). These data suggest that caveolae-mediated endocytosis is the primary cellular uptake pathway for SP/siRNA, whereas clathrin-mediated endocytosis and macropinocytosis play secondary roles. In contrast, clathrin-mediated endocytosis plays a predominant role in LF uptake and caveolae-mediated endocytosis constitutes a minor pathway.

4 Discussion

siRNAs have great potential as gene-specific therapeutic agents for the treatment of a wide range of diseases[7]. However, clinical translation of siRNA is significantly hampered by poor delivery of siRNA[7]. Previously, Span 40 has been formulated with Cholesteryl 3β-N-(dimethylaminoethyl)carbamate hydrochloride (DC-Chol) and 1, 2-distearoyl-sn-glycero-3-phosphoethanolamine-N-[poly-(ethyleneglycol)-2000] (PEG2000-DSPE) to form PEGylated cationic niosomes. The PEGylated cationic niosomes were shown to increase serum stability and cellular uptake of ODN[15]. However, the particle size of the PEGylated cationic noisomes dramatically increased to more than 300 nm after complexing with ODN, undermining their potential for *in vivo* application[23].

The present work explored the potential of the non-ionic surfactant, Span 80, co-formulated with DOTAP and TPGS as a delivery system for siRNA. The SP/siRNA formulation was shown to have good colloidal stability (Figure 1) and high siRNA loading even at high NA/SP ratio (1/2.5) and high percentage of TPGS (Figure 2). In addition, the small particle size and moderate surface charge of SP/siRNA complexes (Figure 2) are desirable characteristics that may result in a prolonged blood circulation time[23, 41]. The complexes of SP with 5% TPGS, although showing a larger particle size than complexes of SP with 1% TPGS, still remained under 200 nm[42]. The complexes of SP with 5% TPGS could be beneficial for *in vivo* applications by reducing plasma protein binding and avoiding RES uptake due to increased PEGylation density on the particle surface[42, 43].

Cryo-TEM images of the SP/siRNA complexes showed that the complexes were predominantly unilamellar core-shell particles and were distinct from the multilamellar structures of the liposome/siRNA complexes[31, 44]. The multilamellar structures of the liposome/siRNA complexes were formed because the negatively charged siRNA molecules were able to hold adjacent membranes together[44]. The distinct morphology of the SP/siRNA complexes implies that the Span 80 containing membrane may possess very different properties from the lipid bilayer, which might prevent the membranes from forming multilayered structures.

Transfection experiments showed that the SP/siGFP complexes with NA/SP ratio < 1/5 resulted in a significant reduction of GFP expression (Figure 5A). The optimal NA/SP ratio for SP/siRNA complexes was found to be 1/15. Further decreases in the NA/SP ratio did not result in more efficient knockdown of the GFP gene. A similar phenomenon has been observed previously both in polymer-[45] and liposome-[46] mediated siRNA transfection.

Compared to the widely used cationic liposome based transfection reagent LF, SP achieved markedly higher GFP silencing activity in the entire dose range (5~100 nM). SP/siGFP was 5.2-fold more effective in GFP silencing than LF at 40 nM. In addition, the SP/siArom complexes were shown to effectively silence the endogenous aromatase gene showing 77% knockdown in SKBr-3 cells at a siRNA concentration of 40 nM (Figure 6). Furthermore, the high transfection efficiency of this novel vector was accompanied by minimal cytotoxicity (Figure 4). For both GFP and aromatase gene silencing, the activities of SP with 1 % and

5%TPGS were not statistically significant, suggesting a higher percentage of TPGS in the SP formulation did not significantly affect the transfection activity. Because adding more PEGylated lipids to cationic liposomes has been shown to reduce RES clearance[47] and reduce their cytotoxicity[7], SP with higher TPGS percentages may be used to achieve optimal circulation half-time and lower toxicity *in vivo*[41].

The gene silencing activity depends on the cellular trafficking of the complexes. Therefore, an important consideration for designing a delivery system is whether the siRNA payload is efficiently released into the cytosol[48]. Span 80 is known to form a hexagonal II phase at high surfactant concentration[49], therefore, it is believed to promote bilayer destabilization[21] when included at high percentages in nanoparticles. This in turn should facilitate endo/lysosomal escape of siRNA into the cytosol (Figure 7). LF, despite being able to mediate higher uptake of siRNA than SP (Figure 8A), was unable to facilitate its escape from the lysosomal compartment (Figure 7) and as a result was less effective in mediating gene knockdown (Figure 5B and Figure 6). Indeed, using MB as an endosomal release marker, it was shown that SP/siRNA delivered the majority of internalized nucleic acid into the cytosol (Figure 8). The cellular entry mechanism was further investigated by co-treatment of the cells with specific endocytosis pathway inhibitors. SP/siRNA was shown to enter the cell through a combination of caveolae-mediated endocytosis (60%), macropinocytosis (13%) and clathrin-mediated endocytosis (42%); while LF was taken up mainly via clathrin-mediated endocytosis (62%) and partially via caveolae-mediated endocytosis (35%). Transfection vectors that entered the cell through clathrin-mediated endocytosis were usually trapped in endosomes followed by enzymatic degradation in lysosomes[50]. In contrast, caveolae-mediated endocytosis and macropinocytosis were favorable routes for siRNA delivery, due to avoidance of normal lysosomal degradation[50, 51]. Therefore, the cellular uptake mechanism of SP/siRNA facilitated siRNA escape from the endosomes/lysosomes more efficiently (Figure 7), leading to increased gene silencing activity.

To our knowledge, this is the first report on the use of the non-ionic surfactant, Span 80, for delivery of siRNA. We also conducted a direct comparison between 1,2-dioleoyl-sn-glycero-3-phosphoethanolamine (DOPE) and Span 80 by formulating each one along with DOTAP. The data showed that the Span 80 formulation was 6-fold more active than DOPE formulation in siRNA delivery[52]. The surfactant vesicles therefore could prove a superior technology platform for therapeutic siRNA delivery. The present work demonstrates that SPs can be used to deliver siRNA *in vitro*. The next logical step would be to show that the approach is also effective for delivery of siRNA *in vivo*.

5 Conclusions

Here, we report the development of novel surfactant vesicles (SPANosomes) as siRNA delivery vectors. This novel vector, composed of non-ionic surfactant, Span 80, DOTAP, and TPGS, possessed favorable particle size and zeta potential characteristics and mediated efficient cytosolic delivery of siRNA. The optimal formulation of SP/siRNA complexes specifically knocked down 66% and 77% of GFP and aromatase gene expression, respectively in breast cancer cells. The transfection efficiency of SPs was shown to be much greater than that of cationic liposome based transfection reagent, LF. A close examination of the cellular trafficking of siRNA revealed that the superior transfection activity of SP/siRNA might be due to its cellular entry pathways, which avoided lysosomal degradation of SP/siRNA complexes and favored cytosolic delivery of the siRNA. In conclusion, this novel vector constitutes a promising candidate for *in vivo* delivery of siRNA and warrants further investigation.

Acknowledgments

This work was support in part by NSF Grant EEC-0425626, NIH Grant R01 CA135243 and R21CA131832. The authors wish to thank Mike Darby for providing the aromatase inhibitor 7α-APTADD and Bryant Chinung Yung for the valuable comments and suggestions on the manuscript.

REFERENCES

1. Bumcrot D, Manoharan M, Koteliansky V, Sah DW. RNAi therapeutics: a potential new class of pharmaceutical drugs. Nat Chem Biol. 2006; 2(12):711–719. [PubMed: 17108989]
2. Akinc A, Zumbuehl A, Goldberg M, Leshchiner ES, Busini V, Hossain N, Bacallado SA, Nguyen DN, Fuller J, Alvarez R, Borodovsky A, Borland T, Constien R, de Fougerolles A, Dorkin JR, Narayanannair Jayaprakash K, Jayaraman M, John M, Koteliansky V, Manoharan M, Nechev L, Qin J, Racie T, Raitcheva D, Rajeev KG, Sah DW, Soutschek J, Toudjarska I, Vornlocher HP, Zimmermann TS, Langer R, Anderson DG. A combinatorial library of lipid-like materials for delivery of RNAi therapeutics. Nat Biotechnol. 2008; 26(5):561–569. [PubMed: 18438401]
3. Palliser D, Chowdhury D, Wang QY, Lee SJ, Bronson RT, Knipe DM, Lieberman J. An siRNA-based microbicide protects mice from lethal herpes simplex virus 2 infection. Nature. 2006; 439(7072):89–94. [PubMed: 16306938]
4. Judge AD, Robbins M, Tavakoli I, Levi J, Hu L, Fronda A, Ambegia E, McClintock K, MacLachlan I. Confirming the RNAi-mediated mechanism of action of siRNA-based cancer therapeutics in mice. J Clin Invest. 2009; 119(3):661–673. [PubMed: 19229107]
5. Dykxhoorn DM, Palliser D, Lieberman J. The silent treatment: siRNAs as small molecule drugs. Gene Ther. 2006; 13(6):541–552. [PubMed: 16397510]
6. Whitehead KA, Langer R, Anderson DG. Knocking down barriers: advances in siRNA delivery. Nat Rev Drug Discov. 2009; 8(2):129–138. [PubMed: 19180106]
7. Sachin Prakash, Patil; Jeong Wu, Yi; Eun-Kyoung, Bang; Jeon, EM.; Kim, BH. Synthesis and efficient siRNA delivery of polyamine-conjugated cationic nucleoside lipids. Med. Chem. Commun. 2011; 2:505–508.
8. Semple SC, Akinc A, Chen J, Sandhu AP, Mui BL, Cho CK, Sah DW, Stebbing D, Crosley EJ, Yaworski E, Hafez IM, Dorkin JR, Qin J, Lam K, Rajeev KG, Wong KF, Jeffs LB, Nechev L, Eisenhardt ML, Jayaraman M, Kazem M, Maier MA, Srinivasulu M, Weinstein MJ, Chen Q, Alvarez R, Barros SA, De S, Klimuk SK, Borland T, Kosovrasti V, Cantley WL, Tam YK, Manoharan M, Ciufolini MA, Tracy MA, de Fougerolles A, MacLachlan I, Cullis PR, Madden TD, Hope MJ. Rational design of cationic lipids for siRNA delivery. Nat Biotechnol. 2010; 28(2):172–176. [PubMed: 20081866]
9. Hui SW, Langner M, Zhao YL, Ross P, Hurley E, Chan K. The role of helper lipids in cationic liposome-mediated gene transfer. Biophys J. 1996; 71(2):590–599. [PubMed: 8842198]
10. Gao X, Huang L. A novel cationic liposome reagent for efficient transfection of mammalian cells. Biochem Biophys Res Commun. 1991; 179(1):280–285. [PubMed: 1883357]
11. Uchegbu IF, Vyas SP. Non-ionic surfactant based vesicles (niosomes) in drug delivery. Int J Pharm. 1998; 172(1–2):33–70.
12. Paolino D, Cosco D, Muzzalupo R, Trapasso E, Picci N, Fresta M. Innovative bola-surfactant niosomes as topical delivery systems of 5-fluorouracil for the treatment of skin cancer. Int J Pharm. 2008; 353(1–2):233–242. [PubMed: 18191509]
13. Muller D, Foulon M, Bonnemain B, Vandamme TF. Niosomes as carriers of radiopaque contrast agents for X-ray imaging. J Microencapsul. 2000; 17(2):227–243. [PubMed: 10738698]
14. Rentel CO, Bouwstra JA, Naisbett B, Junginger HE. Niosomes as a novel peroral vaccine delivery system. Int J Pharm. 1999; 186(2):161–167. [PubMed: 10486434]
15. Huang Y, Chen J, Chen X, Gao J, Liang W. PEGylated synthetic surfactant vesicles (Niosomes): novel carriers for oligonucleotides. J Mater Sci Mater Med. 2008; 19(2):607–614. [PubMed: 17619962]
16. Huang YZ, Gao JQ, Chen JL, Liang WQ. Cationic liposomes modified with non-ionic surfactants as effective non-viral carrier for gene transfer. Colloids Surf B Biointerfaces. 2006; 49(2):158–164. [PubMed: 16626948]

17. Snider CE, Brueggemeier RW. Potent enzyme-activated inhibition of aromatase by a 7 alpha-substituted C19 steroid. J Biol Chem. 1987; 262(18):8685–8689. [PubMed: 3597393]
18. Zhou C, Yu B, Yang X, Huo T, Lee LJ, Barth RF, Lee RJ. Lipid-coated nano-calcium-phosphate (LNCP) for gene delivery. Int J Pharm. 2010; 392(1–2):201–208. [PubMed: 20214964]
19. Maitani Y, Igarashi S, Sato M, Hattori Y. Cationic liposome (DC-Chol/DOPE=1:2) and a modified ethanol injection method to prepare liposomes, increased gene expression. Int J Pharm. 2007; 342(1–2):33–39. [PubMed: 17566677]
20. Chono S, Li SD, Conwell CC, Huang L. An efficient and low immunostimulatory nanoparticle formulation for systemic siRNA delivery to the tumor. J Control Release. 2008; 131(1):64–69. [PubMed: 18674578]
21. Heyes J, Palmer L, Bremner K, MacLachlan I. Cationic lipid saturation influences intracellular delivery of encapsulated nucleic acids. J Control Release. 2005; 107(2):276–287. [PubMed: 16054724]
22. Yang X, Koh CG, Liu S, Pan X, Santhanam R, Yu B, Peng Y, Pang J, Golan S, Talmon Y, Jin Y, Muthusamy N, Byrd JC, Chan KK, Lee LJ, Marcucci G, Lee RJ. Transferrin receptor-targeted lipid nanoparticles for delivery of an antisense oligodeoxyribonucleotide against Bcl-2. Mol Pharm. 2009; 6(1):221–230. [PubMed: 19183107]
23. Brueggemeier RW, Su B, Sugimoto Y, Diaz-Cruz ES, Davis DD. Aromatase and COX in breast cancer: enzyme inhibitors and beyond. J Steroid Biochem Mol Biol. 2007; 106(1–5):16–23. [PubMed: 17616393]
24. Brueggemeier RW, Su B, Darby MV, Sugimoto Y. Selective regulation of aromatase expression for drug discovery. J Steroid Biochem Mol Biol. 2010; 118(4–5):207–210. [PubMed: 19931613]
25. van der Aa MA, Huth US, Hafele SY, Schubert R, Oosting RS, Mastrobattista E, Hennink WE, Peschka-Suss R, Koning GA, Crommelin DJ. Cellular uptake of cationic polymer-DNA complexes via caveolae plays a pivotal role in gene transfection in COS-7 cells. Pharm Res. 2007; 24(8):1590–1598. [PubMed: 17385010]
26. Mudhakir D, Akita H, Tan E, Harashima H. A novel IRQ ligand-modified nano-carrier targeted to a unique pathway of caveolar endocytic pathway. J Control Release. 2008; 125(2):164–173. [PubMed: 18054812]
27. McNaughton BR, Cronican JJ, Thompson DB, Liu DR. Mammalian cell penetration, siRNA transfection, and DNA transfection by supercharged proteins. Proc Natl Acad Sci U S A. 2009; 106(15):6111–6116. [PubMed: 19307578]
28. Peng M, Yin N, Zhang W. Endocytosis of FcalphaR is clathrin and dynamin dependent, but its cytoplasmic domain is not required. Cell Res. 2010; 20(2):223–237. [PubMed: 19859085]
29. Ozgenc F, Aksu G, Kirkpinar F, Altuglu I, Coker I, Kutukculer N, Yagci RV. The influence of marginal zinc deficient diet on post-vaccination immune response against hepatitis B in rats. Hepatol Res. 2006; 35(1):26–30. [PubMed: 16600672]
30. Heurtault B, Saulnier P, Pech B, Proust JE, Benoit JP. Physico-chemical stability of colloidal lipid particles. Biomaterials. 2003; 24(23):4283–4300. [PubMed: 12853260]
31. Desigaux L, Sainlos M, Lambert O, Chevre R, Letrou-Bonneval E, Vigneron JP, Lehn P, Lehn JM, Pitard B. Self-assembled lamellar complexes of siRNA with lipidic aminoglycoside derivatives promote efficient siRNA delivery and interference. Proc Natl Acad Sci U S A. 2007; 104(42): 16534–16539. [PubMed: 17923669]
32. Sharififar F, Noudeh GD, Khazaeli P, Mirzaei S, Nasrollahosaiani S. Determination of the Toxicity Effect of Sorbitan Esters Surfactants Group on Biological Membrane. J. Biol. Sci. 2009; 9(5):423–430.
33. Geusens B, Lambert J, De Smedt SC, Buyens K, Sanders NN, Van Gele M. Ultradeformable cationic liposomes for delivery of small interfering RNA (siRNA) into human primary melanocytes. J Control Release. 2009; 133(3):214–220. [PubMed: 18973779]
34. Dalby B, Cates S, Harris A, Ohki EC, Tilkins ML, Price PJ, Ciccarone VC. Advanced transfection with Lipofectamine 2000 reagent: primary neurons, siRNA, and high-throughput applications. Methods. 2004; 33(2):95–103. [PubMed: 15121163]
35. Ying B, Campbell R. Optimized Formulation for Liposomal siRNA Delivery to the Tumor Vasculature. AAPS J. 2009; 11:S2. Abstract AM2009.

36. Ruozi B, Montanari M, Vighi E, Tosi G, Tombesi A, Battini R, Restani C, Leo E, Forni F, Vandelli MA. Flow cytometry and live confocal analysis for the evaluation of the uptake and intracellular distribution of FITC-ODN into HaCaT cells. J Liposome Res. 2009; 19(3):241–251. [PubMed: 19694606]
37. Tyagi S, Kramer FR. Molecular beacons: probes that fluoresce upon hybridization. Nat Biotechnol. 1996; 14(3):303–308. [PubMed: 9630890]
38. Chen AK, Behlke MA, Tsourkas A. Efficient cytosolic delivery of molecular beacon conjugates and flow cytometric analysis of target RNA. Nucleic Acids Res. 2008; 36(12):e69. [PubMed: 18503086]
39. Santangelo P, Nitin N, Bao G. Nanostructured probes for RNA detection in living cells. Ann Biomed Eng. 2006; 34(1):39–50. [PubMed: 16463087]
40. Zhou C, Mao Y, Lee LJ, Lee RJ. Quantitative analysis of intracellular and cytoplasmic siRNA delivery by SPANosomes. AAPS J. 2010; 12:S2. Abstract T2073.
41. Ae-June, Wang; Pei-Lin, Wang; Shin-Jr, Lu. Long circulating liposome. U.S. Patent. 200810166403A1. 2008.
42. Li W, Szoka FC Jr. Lipid-based nanoparticles for nucleic acid delivery. Pharm Res. 2007; 24(3): 438–449. [PubMed: 17252188]
43. Juliano R, Bauman J, Kang H, Ming X. Biological barriers to therapy with antisense and siRNA oligonucleotides. Mol Pharm. 2009; 6(3):686–695. [PubMed: 19397332]
44. Weisman S, Hirsch-Lerner D, Barenholz Y, Talmon Y. Nanostructure of cationic lipid-oligonucleotide complexes. Biophys J. 2004; 87(1):609–614. [PubMed: 15240493]
45. Breunig M, Hozsa C, Lungwitz U, Watanabe K, Umeda I, Kato H, Goepferich A. Mechanistic investigation of poly(ethylene imine)-based siRNA delivery: disulfide bonds boost intracellular release of the cargo. J Control Release. 2008; 130(1):57–63. [PubMed: 18599144]
46. Zhang Y, Li H, Sun J, Gao J, Liu W, Li B, Guo Y, Chen J. DC-Chol/DOPE cationic liposomes: A comparative study of the influence factors on plasmid pDNA and siRNA gene delivery. Int J Pharm. 2010
47. Malam Y, Loizidou M, Seifalian AM. Liposomes and nanoparticles: nanosized vehicles for drug delivery in cancer. Trends Pharmacol Sci. 2009; 30(11):592–599. [PubMed: 19837467]
48. Medina-Kauwe LK, Xie J, Hamm-Alvarez S. Intracellular trafficking of nonviral vectors. Gene Ther. 2005; 12(24):1734–1751. [PubMed: 16079885]
49. Wei-Qing, Zhou; Ting-Yue, Gu; Zhi-Guo, Su; Ma, G-H. Synthesis of macroporous poly(styrene-divinyl benzene) microspheres by surfactant reverse micelles swelling method. Polymer. 2007; 48:1981–1988.
50. Khalil IA, Kogure K, Akita H, Harashima H. Uptake pathways and subsequent intracellular trafficking in nonviral gene delivery. Pharmacol Rev. 2006; 58(1):32–45. [PubMed: 16507881]
51. Love KT, Mahon KP, Levins CG, Whitehead KA, Querbes W, Dorkin JR, Qin J, Cantley W, Qin LL, Racie T, Frank-Kamenetsky M, Yip KN, Alvarez R, Sah DW, de Fougerolles A, Fitzgerald K, Koteliansky V, Akinc A, Langer R, Anderson DG. Lipid-like materials for low-dose, in vivo gene silencing. Proc Natl Acad Sci U S A. 2010; 107(5):1864–1869. [PubMed: 20080679]
52. Zhou C, Lee LJ, Lee RJ. Cellular pharmacokinetics (PK) and target gene knockdown of surfactant- and lipid-based nanocarriers (NCs) of siRNA. AAPS J. 2011; 13:S1. Abstract W3028.

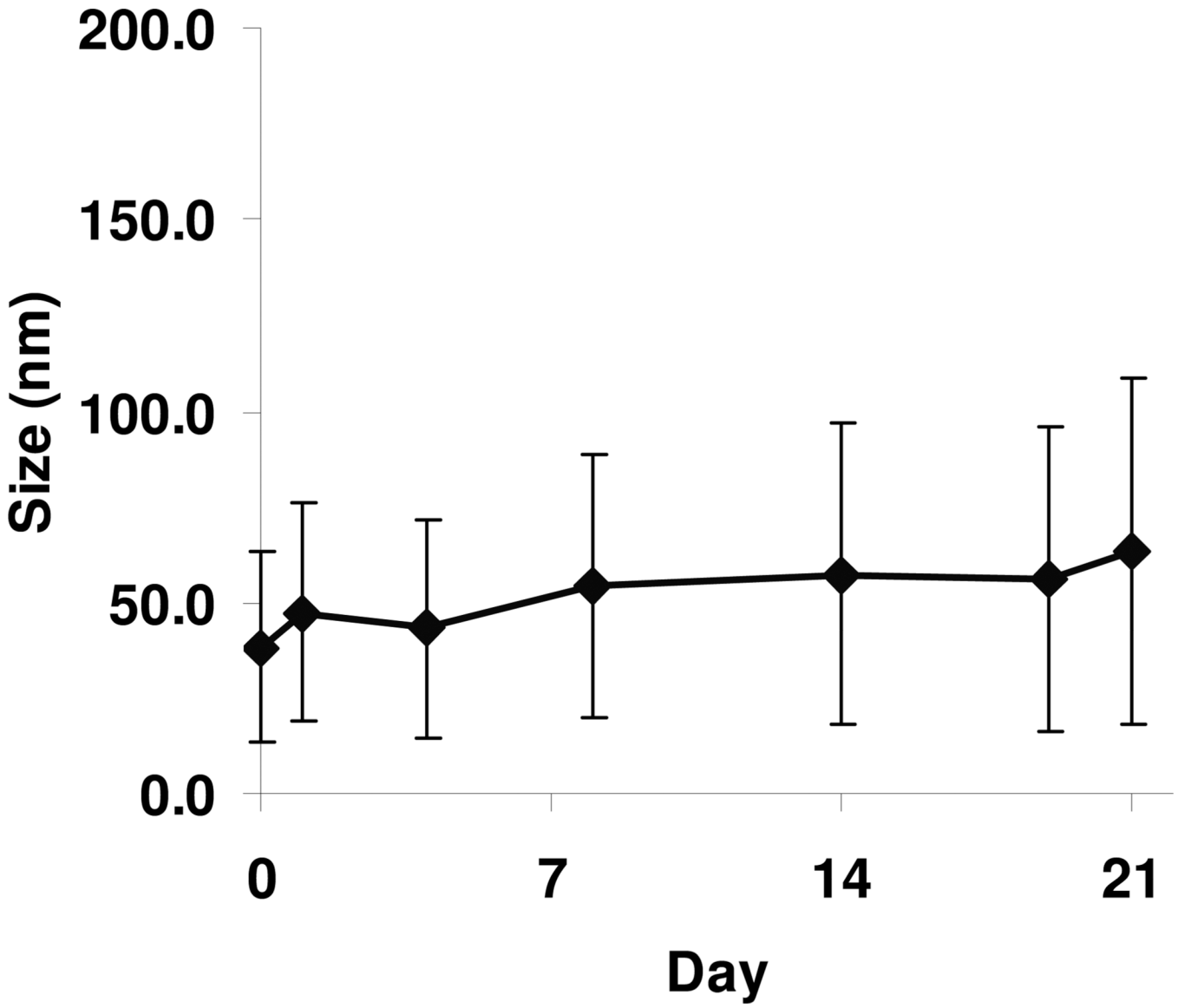

Figure 1. Particle size and colloidal stability of SPs

The particle size (diamond) and size distribution width (error bar) of SPs remained stable for up to 3 weeks after synthesis and storage at 4°C.

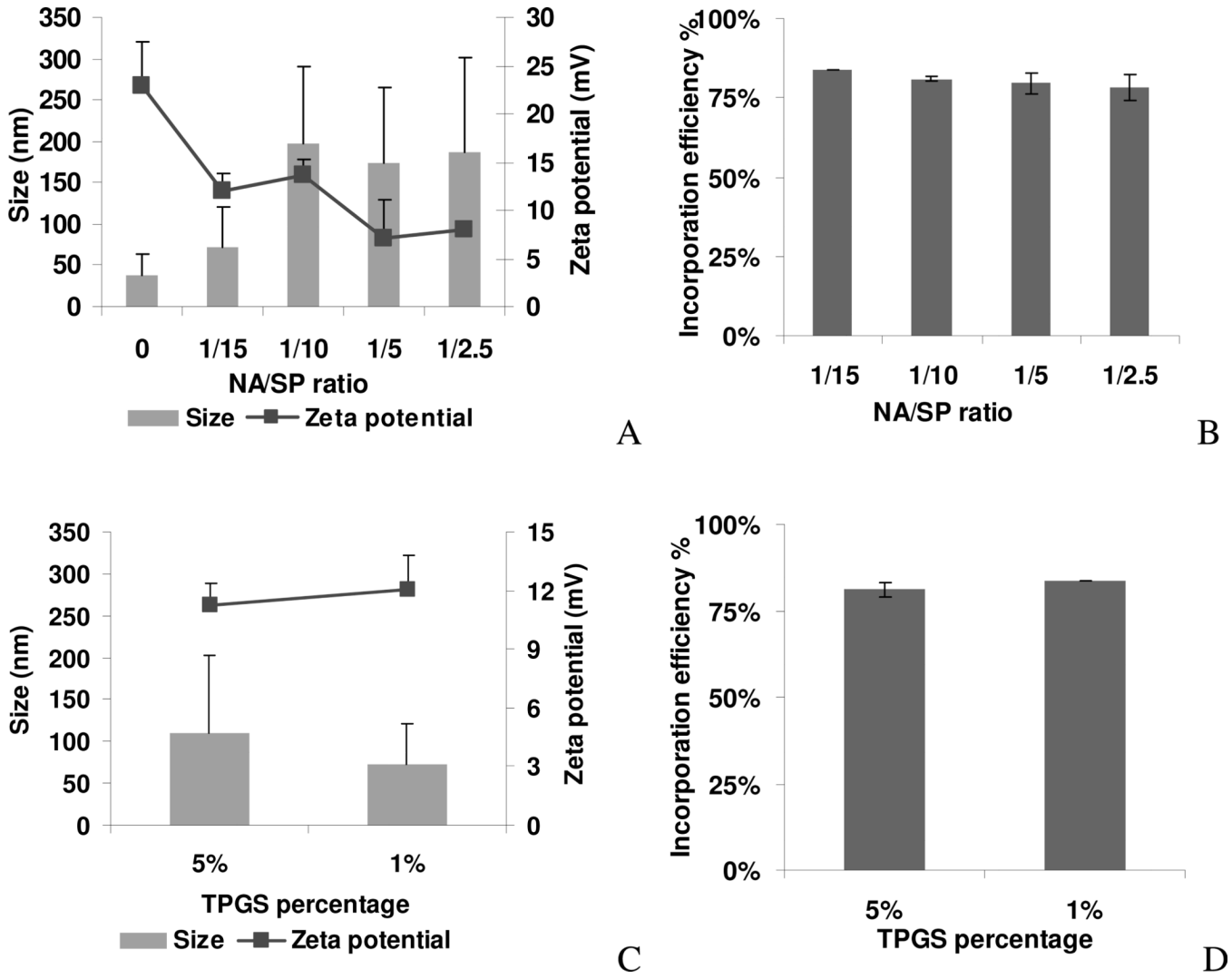

Figure 2. Optimization of the SP formulation

SP with 1% TPGS was used to study the effect of nucleic acid/SPANosomes (NA/SP, w/w) ratios on (A) zeta potential ± S.D. (n=3) and particle size ± S.D. of size distribution, and (B) incorporation efficiency ± S.D. of SP/siRNA complexes (n=3). The effect of TPGS percentage on the (C) particle size, zeta potential, and (D) incorporation efficiency of SP/siRNA complexes.

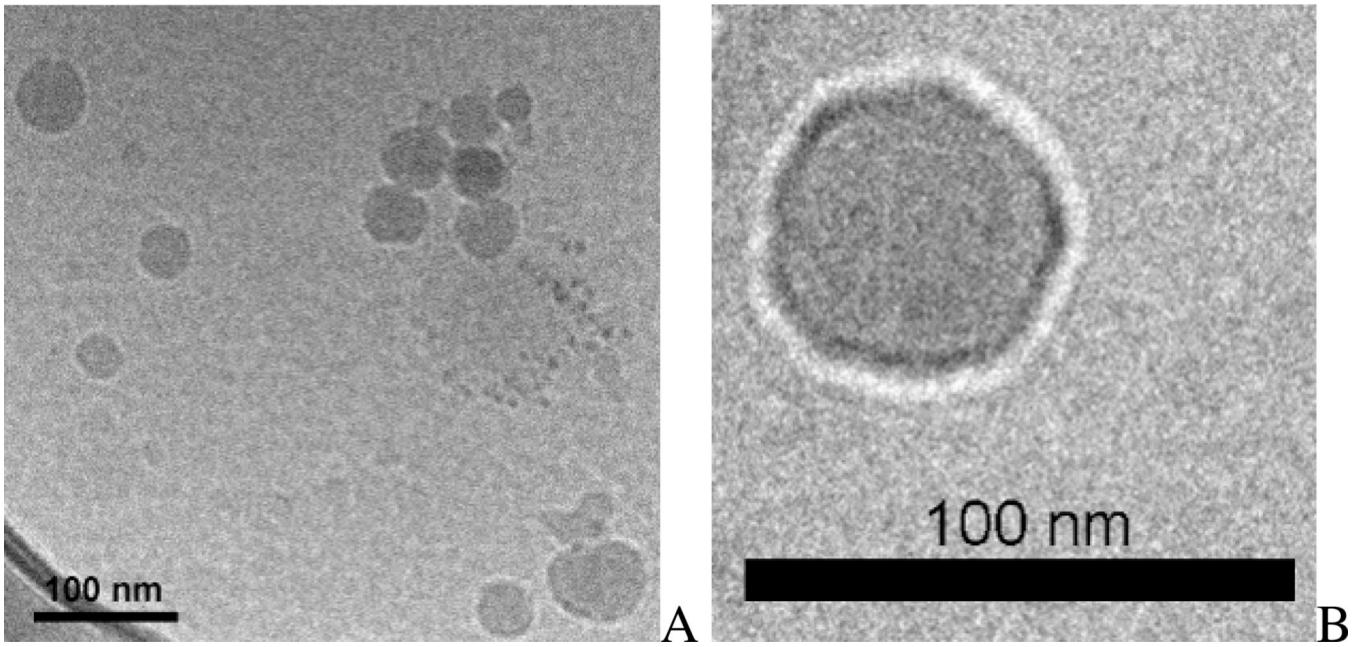

Figure 3. Cryo-TEM photographs of SP/siRNA complexes

The SP with 1% TPGS was complexed with siRNA at the NA/SP ratio of 1/15 for cryo-TEM imaging. Bar=100 nm.

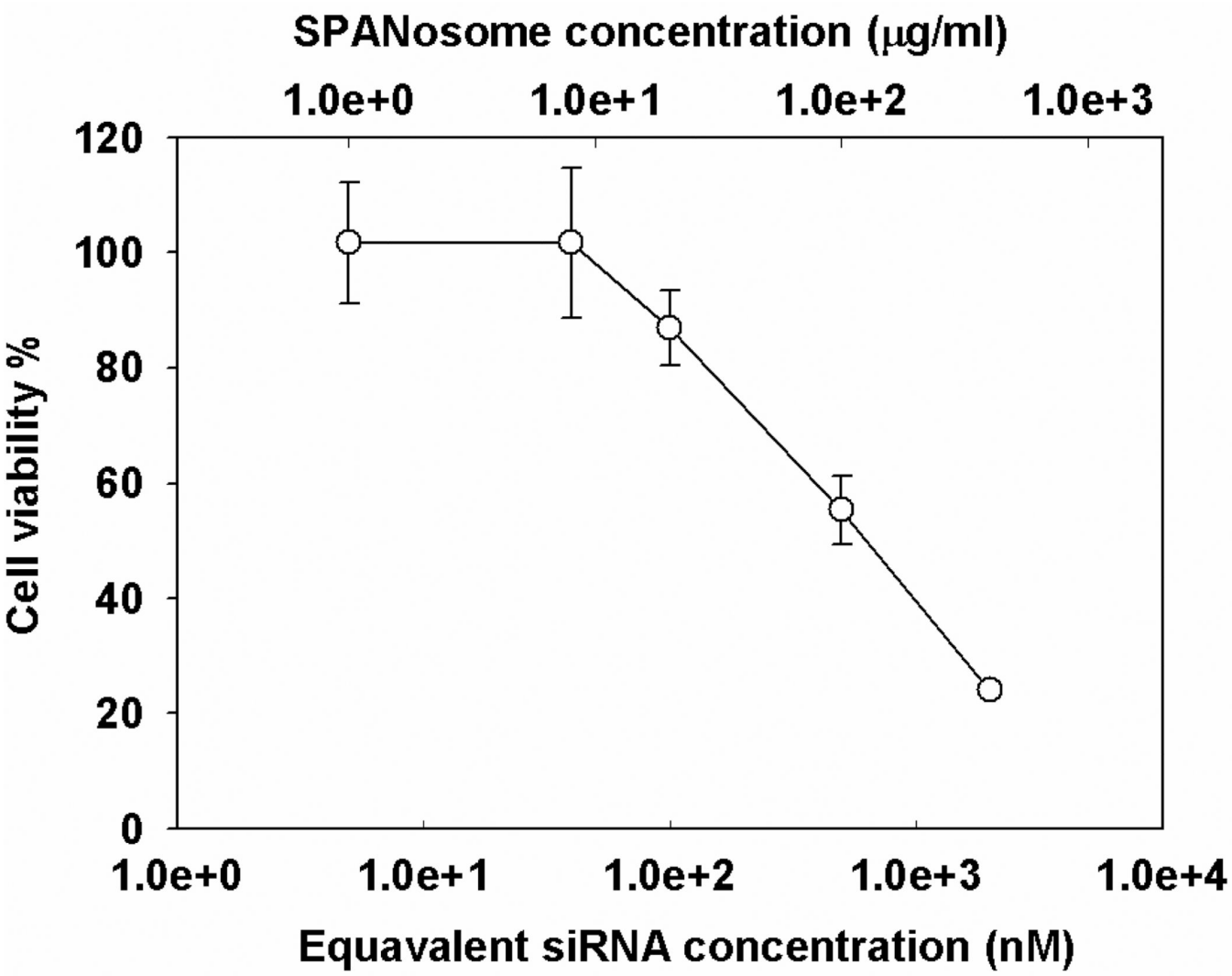

Figure 4. Cytotoxicity of SPs

Vehicle related cytotoxicity of SPs in MDA-MB-231 cells as a function of SP concentration. The cells were treated with increasing SP concentration for 24 h and cell viability was measured by the MTS assay. Equivalent siRNA concentration was calculated by SP concentration (g/L) × 15 / molecular weight of siRNA (g/mol). Values represent the mean ± S.D. (n=3).

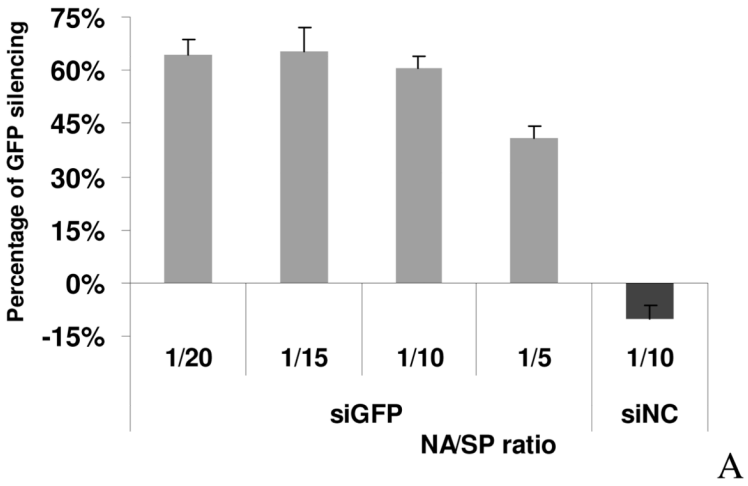

A

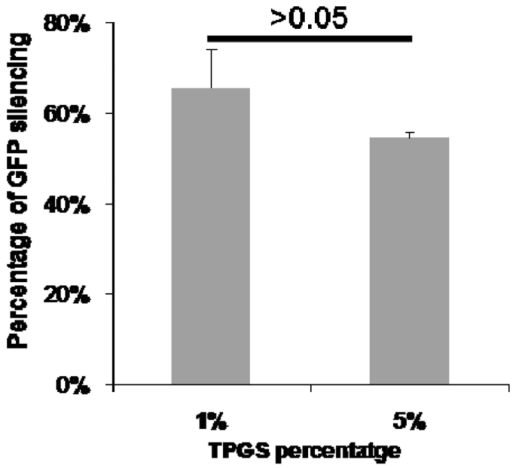

B

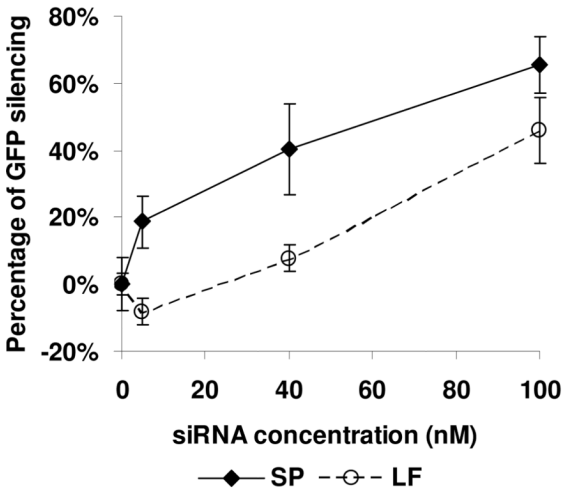

C

Figure 5. GFP silencing activity of the SP/siRNA complexes

(A) GFP silencing activity of the SP/siGFP complexes at the 100 nM siRNA level with different NA/SP ratios. (B) GFP silencing activity of the SP/siRNA complexes with 1% and 5% TPGS in the SP formulation at the 100 nM siRNA level (NA/SP=1/15). (C) GFP silencing activity of the SP/siRNA and LF/siRNA complexes with different siRNA concentrations at the optimal NA/SP ratio (1/15). GFP expression was quantified by flow cytometry analysis. Values represent the mean ± S.D. (n=3).

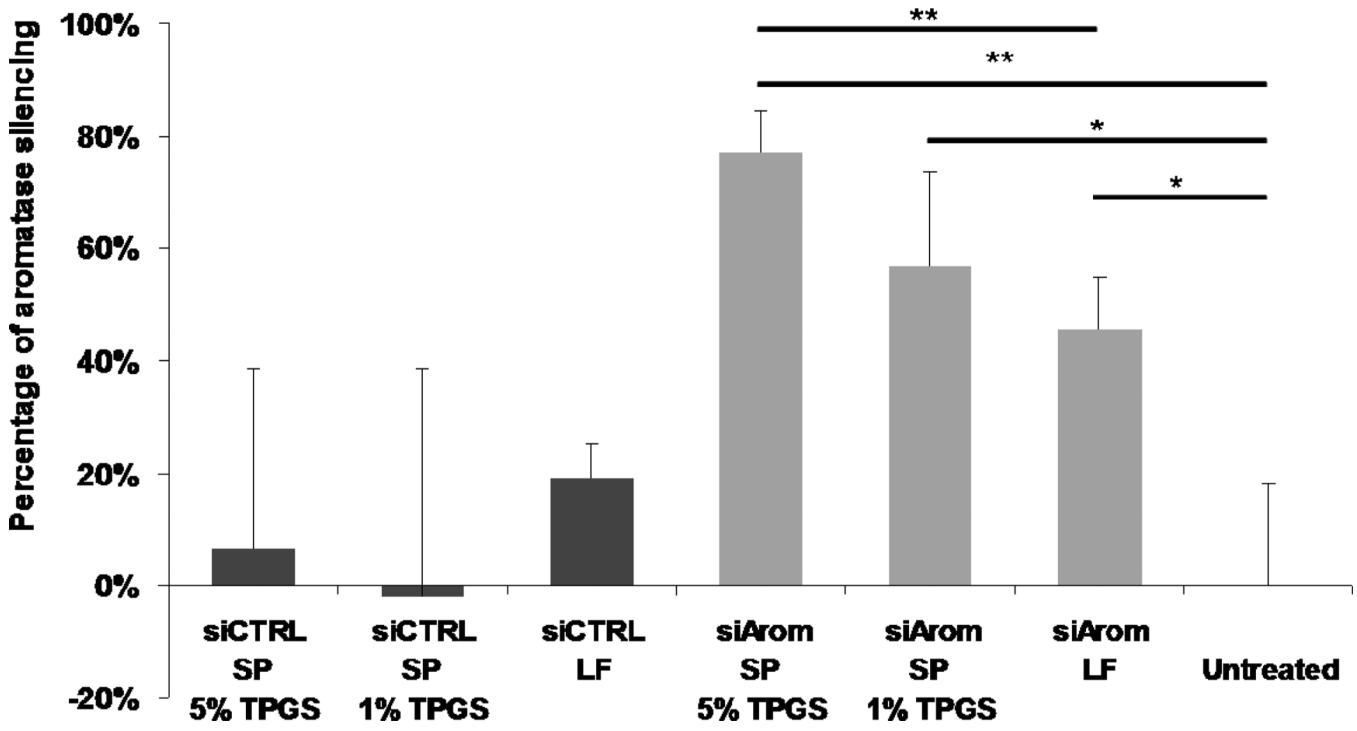

Figure 6. Aromatase knockdown by the SP/siArom complexes

Aromatase silencing activity of SP and LF was measured in the SKBr-3 cell line at the 40 nM siRNA level. Aromatase activity was determined by ^3H_2O release assay. The aromatase activity was normalized to the total amount of DNA to obtain the normalized aromatase level. Values are relative to untreated control and represent the mean ± S.D. (n=3). * $p<0.05$, ** $p<0.01$.

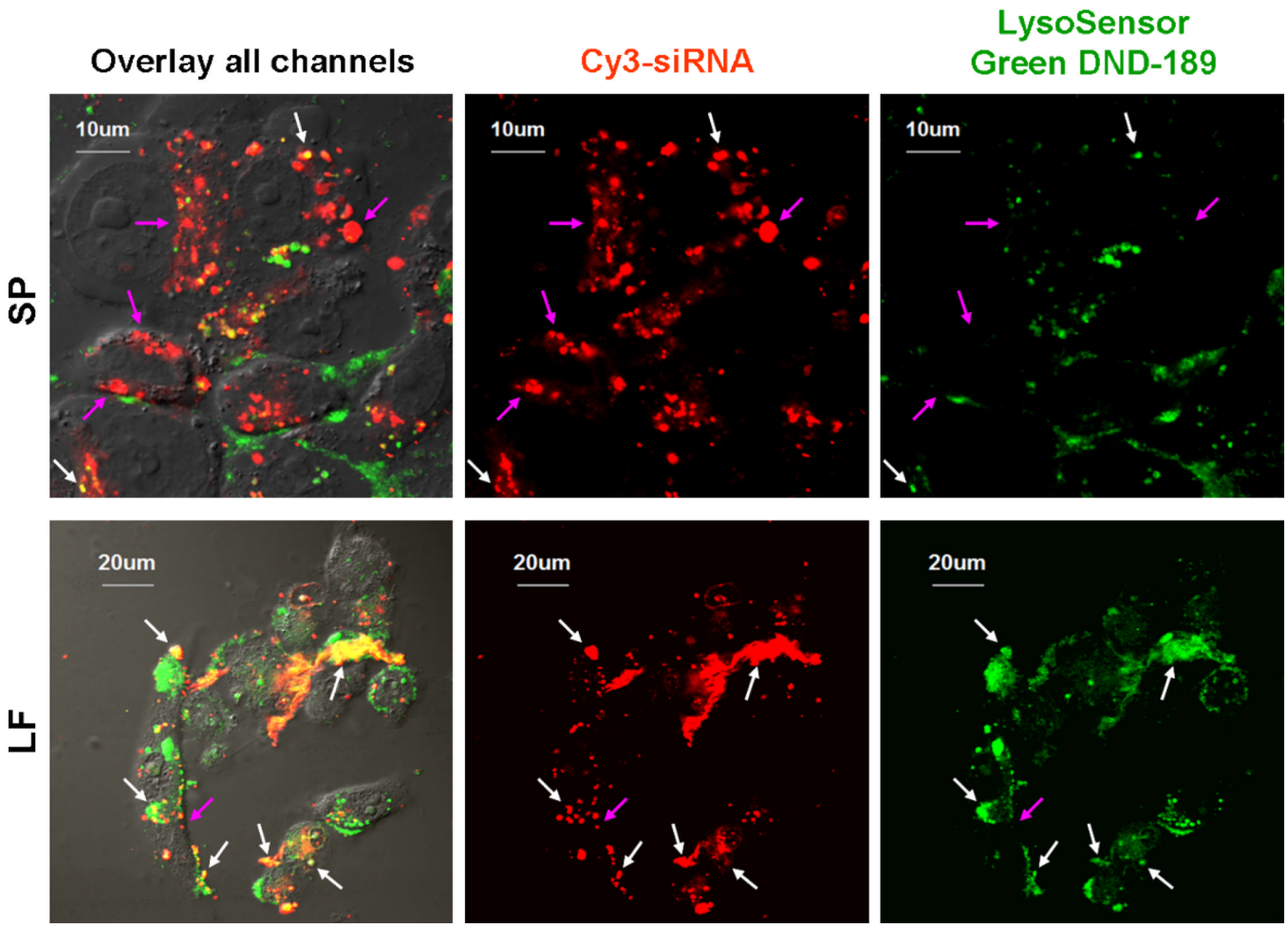

Figure 7. Subcellular localization of siRNA

MDA-MB-231 cells on glass coverslips were incubated with complexes containing 100 nM Cy3-siRNA and 2 μM LysoSensor Green DND-189 for 1 h at 37 °C. After treatment, the cells were washed three times with PBS before live-cell imaging on a confocal microscopy. Yellow dots (white arrow) indicated co-localization of Cy3-siRNA and LysoSensor, suggesting the complexes were trapped in lysosomal compartment. Red dots (purple arrow) indicated Cy3-siRNA that had escaped the lysosomes. LysoSensor Green DND-189 is a fluorescent pH indicator that partitions into lysosomes and is only fluorescent at low pH.

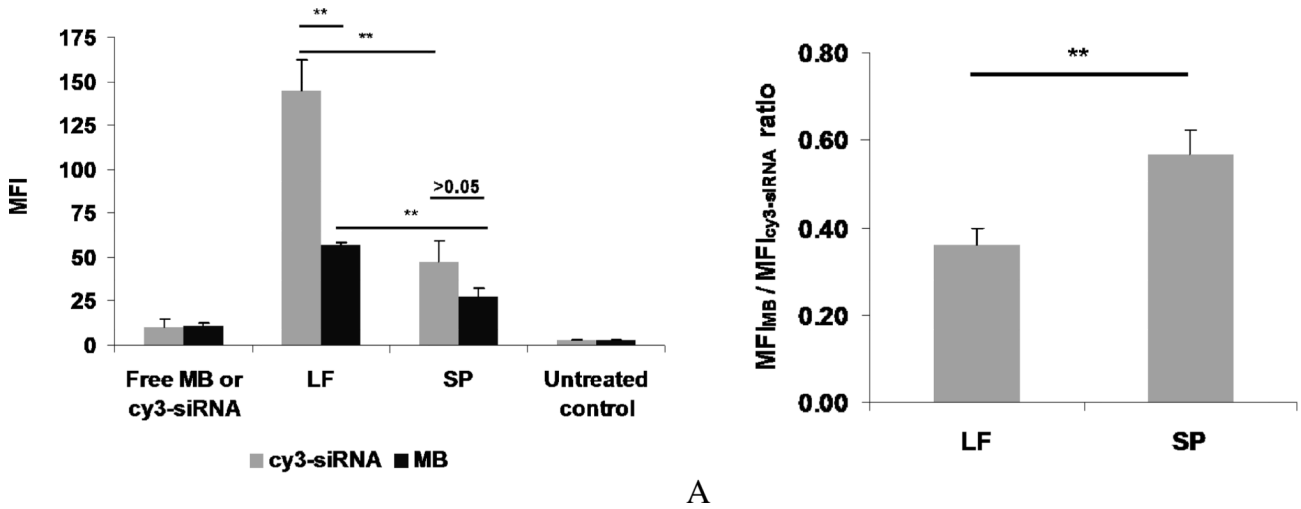

Figure 8. Flow cytometry analyses of SP and LF mediated uptake of Cy3-siRNA and MB

Cy3-siRNA and MB transfection were performed as described in Figure 7. After 2 h treatment, MDA-MB-231 cells were washed 3 times by PBS and fixed with 4% formalin. Fluorescent intensity in cells was measured by flow cytometry. (A) The MFI (mean fluorescent intensity) was used to quantify delivery of Cy3-siRNA and MB. (B) The ratio of the MFI of MB to that of Cy3-siRNA was used to determine the extent of cytosolic release of the siRNA by SP and LF. Values are represented as the mean ± S.D. (n = 3). * $p < 0.05$, ** $p<0.01$.

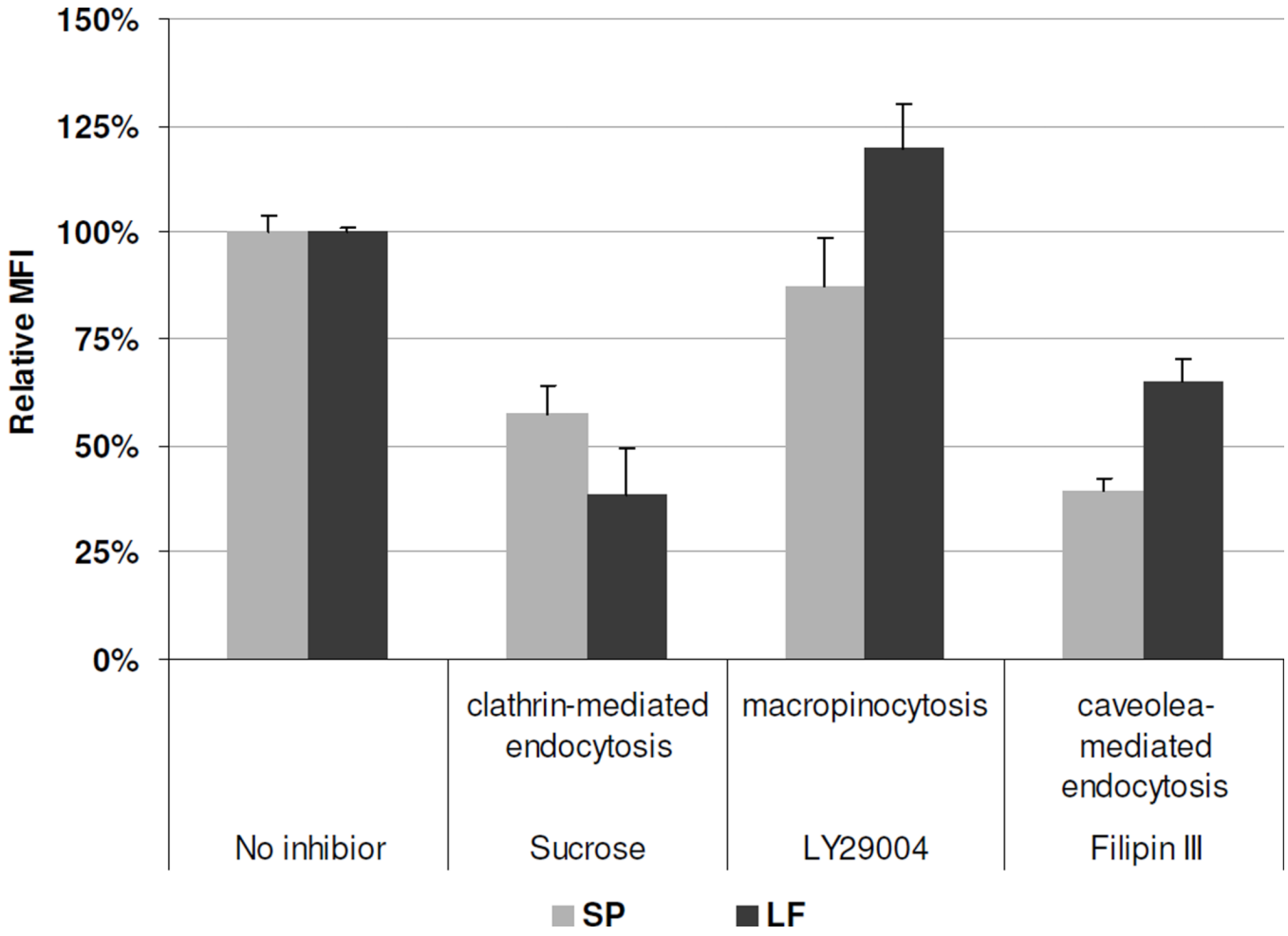

Figure 9. Mechanism of SP and LF mediated siRNA transfection

MDA-MB-231 cells were pre-incubated with or without an inhibitor of clathrin-mediated endocytosis (sucrose, 0.4 M), macropinocytosis (LY29004, 50 μM), and caveolae-mediated endocytosis (filipin III, 5 μg/ml) for 1 h at 37 °C. These cells were then transfected with 100 nM SP or LF/FAM-siRNA complexes in the absence or presence of the inhibitors at the same concentration for 1 h. After transfection, the cells were washed 3 times with PBS, fixed and analyzed by flow cytometry. MFI data was normalized to the cells treated without any inhibitor (100% relative MFI).

Table 1

Particle size and zeta potential of SP formulation.

Lipid composition (mol ratio)	Particle size ± S.D. of size distribution (nm)	Zeta potential ± S.D. (mV)
DOTAP/Span 80/TPGS =50:49:1	38.4±25.1	22.9±4.61
DOTAP/Span 80/TPGS =50:45:5	23.6±17.8	33.5±0.87